ELSEVIER

Journal of Alloys and Compounds 386 (2005) 26–34

Journal of ALLOYS AND COMPOUNDS

www.elsevier.com/locate/jallcom

Hydrogen-induced changes in crystal structure and magnetic properties of the Zr_3MO_x (M = Fe, Co) phases

I.Yu. Zavaliy [a,*], R.V. Denys [a], R. Černý [b], I.V. Koval'chuck [a], G. Wiesinger [c], G. Hilscher [c,1]

[a] *Physico-Mechanical Institute of the NAS of Ukraine, 5 Naukova Str., Lviv 79601, Ukraine*
[b] *Laboratory of Crystallography, University of Geneva, 24 Quai Ernest-Ansermet, CH-1211 Geneva 4, Switzerland*
[c] *Institute of Solid State Physics, TU Vienna, Wiedner Hauptstrasse 8-10, A-1040 Vienna, Austria*

Received 14 May 2004; accepted 16 May 2004

Abstract

It is shown that the oxygen-stabilised compounds $Zr_3Fe(Co)O_x$ ($x = 0$–1.0) interact with hydrogen at ambient temperature and pressure forming saturated hydrides with filled Re_3B type structure. The hydrogen storage capacity decreases with increasing oxygen content from 6.7 H/f.u. for Zr_3Fe down to 5.35 H/f.u. for $Zr_3FeO_{1.0}$ and from 6.9 H/f.u. for Zr_3Co down to 5.3 H/f.u. for $Zr_3CoO_{1.0}$. A small change of the unit cell volumes for the $Zr_3Fe(Co)O_x$ parent compounds and a substantial increase of these parameters for the corresponding saturated hydrides were observed with increasing oxygen content. The partial hydrogen-induced lattice expansion, ΔV/at. H, increases from 2.25 Å^3 for $Zr_3FeH_{6.7}$ up to 3.38 Å^3 for $Zr_3FeO_{1.0}H_{5.35}$ and from 2.08 Å^3 for $Zr_3CoH_{6.9}$ up to 3.25 Å^3 for $Zr_3CoO_{1.0}H_{5.3}$. Rietveld refinement using neutron powder diffraction data for $Zr_3FeO_{0.4}D_{6.25}$ showed a distribution of deuterium atoms and a redistribution of oxygen atoms from octahedral to tetrahedral sites in a similar way as in $Zr_3NiO_xD_y$. Both ^{57}Fe Mössbauer spectroscopy and magnetic susceptibility measurements of Fe-containing hydrides indicated weak hydrogen-induced magnetic ordering at low temperatures. The ordering temperatures of $Zr_3FeO_{0.2}H_{6.52}$ and $Zr_3FeO_{0.6}H_{6.25}$ are 105 and 140 K, respectively.

Keywords: Hydrogen storage materials; Zr-based alloys; X-ray diffraction; Neutron diffraction; Magnetic properties

1. Introduction

A_3B phases with the Re_3B type structure, formed in zirconium and hafnium-based systems dissolve oxygen up to the composition A_3BO (Zr_3Fe, Zr_3Co) [1] or can be stabilised by oxygen, when such compound does not exist in the binary system (Zr_3NiO and Hf_3NiO) [2]. The oxygen atom occupies the octahedral void in the Re_3B structure. Hydrogenation properties of $Zr_3Fe(Co)$ phases and their crystal structure were investigated in detail [3–5]. Studies of Zr_3FeH_x hydrides by Mössbauer spectroscopy performed previously by Aubertin et al. [6] showed the presence of hydrogen-induced magnetic ordering upon cooling to 4.2 K. However, neither the type of magnetic ordering nor the transition temperature has been determined.

Hydrogenation properties of an oxygen-stabilised compound and its crystal structure were studied recently for $Zr_3NiO_xD_y$ [7,8]. Reversible hydrogen-induced redistribution of oxygen atoms in the crystal structure and the inverse dependence of the hydrogen absorption capacity on the oxygen content were observed. The aim of this work was a study of the crystal structure and magnetic properties of oxygen-stabilised Zr_3MO_x compounds and their hydrides, for M = Fe, Co.

2. Experimental

Zr_3MO_x (M = Fe, Co; $x = 0.2$, 0.4, 0.6, 0.8, 1.0) alloys were prepared from pure metals by arc melting in a purified argon atmosphere on a water-cooled copper hearth. Oxygen was introduced into the alloys in the form of the oxide ZrO_2. Further homogenisation of the as-cast samples was performed by annealing at 800 °C for 400 h. Two batches of samples were prepared: first, for hydrogenation and X-ray

* Corresponding author. Tel.: +380-322-654833; fax: +380-322-649427.
E-mail address: zavaliy@ipm.lviv.ua (I.Yu. Zavaliy).
[1] Tel.: +43-1-58801-13130; fax: +43-1-58801-13199.

0925-8388/$ – see front matter © 2004 Elsevier B.V. All rights reserved.
doi:10.1016/j.jallcom.2004.05.064

diffraction characterisation of $Zr_3Fe(Co)O_x$ (~2 g each), and second, for neutron diffraction studies of $Zr_3FeO_{0.4}$ (~6 g). Characterisation of the parent alloys and their hydrides was carried out by the X-ray powder diffraction (diffractometer DRON-3.0; Cu Kα radiation) and by high resolution X-ray powder diffraction (Bruker D8 diffractometer; Cu $K\alpha_1$ radiation). Crystal structure studies of the $Zr_3FeO_{0.4}D_{6.52}$ deuteride were performed using X-ray as well as neutron powder diffraction (Paul Scherrer Institute, diffractometer HRPT, high resolution mode, wavelength 1.494 Å). The lattice parameters were refined using the program CSD [9]. The crystal structure of the selected hydrides and the $Zr_3FeO_{0.4}D_{6.52}$ deuteride was refined by Rietveld method using the program FullProf [10].

The hydrogen/deuterium absorption characteristics were determined by a standard volumetric technique. Hydrogen/deuterium was injected into a stainless steel reactor containing a preliminary activated sample (300–400 °C for 0.5 h in ~1 Pa vacuum). An exposure of the samples to a hydrogen/deuterium pressure of 0.1–0.12 MPa for 5−10 h was sufficient for achieving saturation of the alloys with hydrogen/deuterium.

The ^{57}Fe Mössbauer spectra were recorded in transmission geometry at room and liquid helium temperatures using a conventional constant acceleration type spectrometer with a ^{57}Co source in a Rh matrix. The data were analysed by fitting sets of Lorentzian lines to the experimental points. The isomer shift values are given relative to the source material. Magnetisation measurements have been performed on powdered specimens with a SQUID magnetometer in fields up to 6 T.

3. Results and discussion

3.1. Synthesis and crystal structure of parent compounds and their hydrides

The formation of the intermetallic phases Zr_3FeO_x and Zr_3CoO_x was confirmed in the homogeneity range of $x = 0$–1.0. Only traces of α-Zr and $Zr_4Fe_2O_x$ (in Fe-containing alloys) and α-Zr and ZrCo (in Co-containing alloys) were observed in the synthesised samples. The refinement of the crystal structure of the parent compounds $Zr_3Fe(Co)O_x$ (samples from the first batch, $x = 0.2$, 0.4, 0.6, 0.8, 1.0) has confirmed the partially filled Re_3B type structure. The lattice parameters of the main phase (weight fraction higher than 90 %) for all studied samples are presented in Table 1. Hydrides of these samples were characterised by the partially filled Re_3B type structure of the metal–oxygen sublattice. The corresponding lattice parameters as well as hydrogen storage capacity are collected in Table 1. It has been observed that the insertion of oxygen atoms leads to a very slight decrease (~0.5%) of the cell volume of the parent phase Zr_3CoO_x in the range $x = 0$–1.0 and small changes (without monotonic tendency) of the cell volume for Zr_3FeO_x (Fig. 1b). It has been observed that the hydrogen-induced lattice expansion of the saturated hydrides increases substantially with the increasing oxygen content while the hydrogen content decreases, which is demonstrated in Fig. 1 by the plots of V_{parent}, $V_{hydride}$, H/M and ΔV/at.H as a function of the O content. The oxygen dependence observed for the $Zr_3Fe(Co)O_xH_y$ hydrides is the same as that obtained for $Zr_3NiO_xH_y$ [7,8].

Table 1
Lattice parameters of parent and hydrogenated Zr_3FeO_x and Zr_3CoO_x compounds from Rietveld refinement (space group Cmcm)

Nominal composition	a (Å)	b (Å)	c (Å)	V (Å^3)	H/M ratio	ΔV/at.H (Å^3)
Zr_3Fe [4]	3.324(2)	10.974(5)	8.821(3)	321.7(1)		
$Zr_3FeH_{6.7}$ [4]	3.5803(3)	11.059(1)	9.6486(8)	382.03(9)	1.73	2.25
$Zr_3FeO_{0.2}$	3.3233(8)	11.028(3)	8.820(2)	323.2(2)		
$Zr_3FeO_{0.2}H_{6.52}$	3.5871(6)	11.123(2)	9.694(2)	386.8(2)	1.63	2.44
$Zr_3FeO_{0.4}$	3.31841(5)	11.0722(2)	8.7995(1)	323.311(8)		
$Zr_3FeO_{0.4}H_{6.40}$	3.56914(7)	11.2356(2)	9.7195(2)	389.76(1)	1.60	2.60
$Zr_3FeO_{0.6}$	3.31731(3)	11.0948(1)	8.78458(9)	323.315(5)		
$Zr_3FeO_{0.6}H_{6.25}$	3.5482(1)	11.3064(4)	9.7452(3)	390.95(2)	1.56	2.72
$Zr_3FeO_{0.8}$	3.3326(8)	11.134(1)	8.728(4)	323.8(1)		
$Zr_3FeO_{0.8}H_{5.68}$	3.527(1)	11.452(1)	9.745(3)	393.7(1)	1.42	3.08
$Zr_3FeO_{1.0}$	3.3228(5)	11.137(2)	8.723(2)	322.8(1)		
$Zr_3FeO_{1.0}H_{5.35}$	3.506(1)	11.504(2)	9.796(4)	395.1(2)	1.34	3.38
Zr_3Co [5]	3.277(3)	10.904(4)	8.990(2)	321.3(2)		
$Zr_3CoH_{6.9}$ [5]	3.5959(1)	10.9734(3)	9.5961(3)	378.65(3)	1.73	2.08
$Zr_3CoO_{0.2}$	3.2864(4)	10.947(1)	8.895(1)	321.0(1)		
$Zr_3CoO_{0.2}H_{6.60}$	3.559(1)	11.126(4)	9.572(4)	379.1(4)	1.65	2.20
$Zr_3CoO_{0.4}$	3.2960(2)	10.9872(6)	8.8575(6)	320.78(7)		
$Zr_3CoO_{0.4}H_{6.30}$	3.5479(3)	11.2006(9)	9.6243(7)	382.46(9)	1.58	2.45
$Zr_3CoO_{0.6}$	3.30541(3)	11.00988(9)	8.81106(8)	320.654(5)		
$Zr_3CoO_{0.6}H_{5.95}$	3.51600(9)	11.3388(3)	9.6590(3)	385.08(2)	1.49	2.71
$Zr_3CoO_{0.8}$	3.31021(4)	11.0204(1)	8.7790(1)	320.258(6)		
$Zr_3CoO_{0.8}H_{5.65}$	3.49761(4)	11.4103(1)	9.6881(1)	386.640(9)	1.41	2.94
$Zr_3CoO_{1.0}$	3.3132(2)	11.0285(5)	8.7449(4)	319.54(3)		
$Zr_3CoO_{1.0}H_{5.30}$	3.4813(3)	11.4729(9)	9.7254(7)	388.44(5)	1.33	3.25

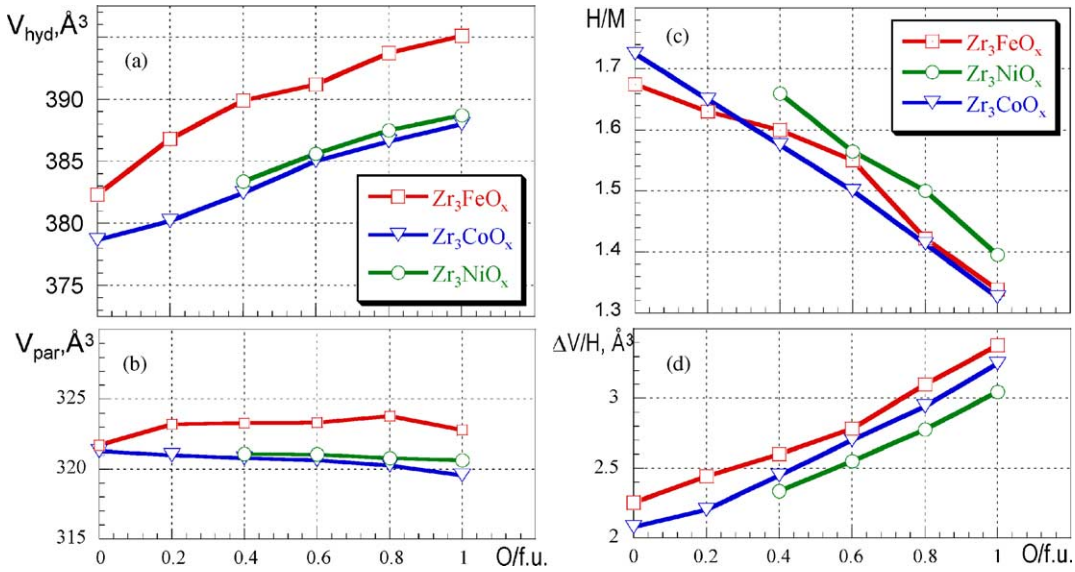

Fig. 1. Unit cell volumes of Zr_3MO_x (M = Fe, Co, Ni) hydrides (a) and parent compounds (b), hydrogen absorption capacity, H/M (c) and the partial hydrogen-induced expansion of the unit cell (d) as a function of the oxygen content (O/f.u.). The results for the Ni containing compounds were taken from [7].

As a typical example the powder patterns of the parent compounds $Zr_3Fe(Co)O_{0.6}$ and the corresponding hydrides experimentally observed, can be compared in Fig. 2 with the calculated spectra and the differential data. The corresponding crystallographic parameters are collected in Table 2. The refinement has confirmed also the occupation of the octahedral interstice O by the oxygen atoms, and has shown that the refined oxygen contents (see Table 2) agree within the experimental error with the nominal composition as obtained from the amount of ZrO_2 inserted in the samples during the synthesis. The crystal structure refinement of the $Zr_3Fe(Co)O_{0.6}H_x$ hydrides confirmed the oxygen atom redistribution from octahedral to tetrahedral interstices, recently observed during the hydrogenation of Zr_3NiO_x [7].

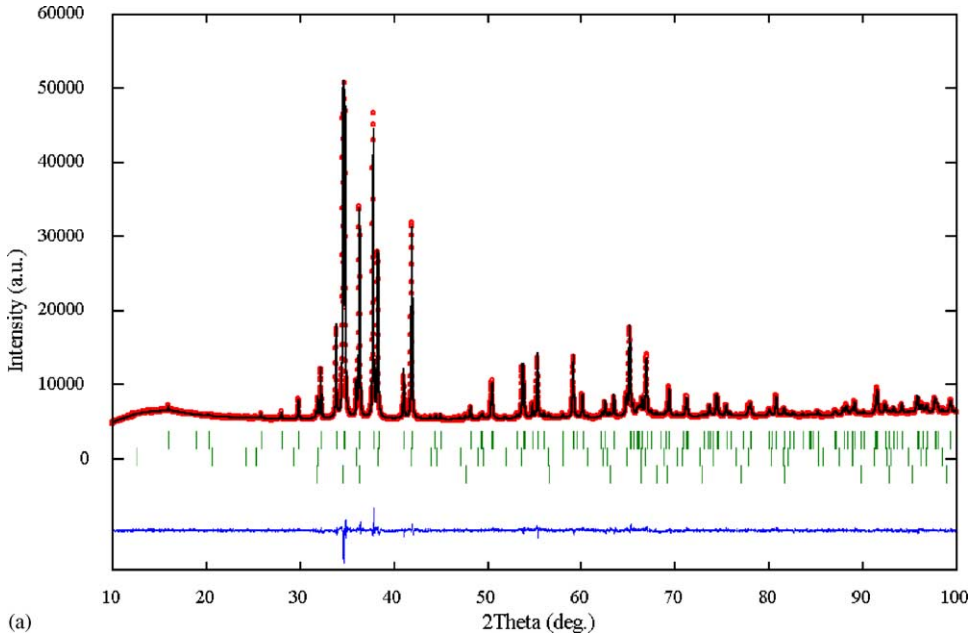

Fig. 2. Observed (points), calculated (line) and difference (lower line) X-ray powder diffraction patterns for the: (a) $Zr_3FeO_{0.6}$ alloy-constituent phases (the vertical bars indicate the position of their Bragg peaks, from top to bottom): $Zr_3FeO_{0.6}$ (90.4(3) wt.%), $Zr_4Fe_2O_x$ (7.58(8) wt.%) and α-Zr (2.07(7) wt.%); (b) hydrogenated $Zr_3FeO_{0.6}$ alloy-constituent phases: $Zr_3FeO_{0.6}H_{6.25}$ (91.1(5) wt.%), $Zr_4Fe_2O_xH_y$ (7.3(2) wt.%) and ZrH_2 (1.6(1) wt.%); (c) $Zr_3CoO_{0.6}$ alloy-constituent phases: $Zr_3CoO_{0.6}$ (96.4(5) wt.%), ZrCo (1.82(9) wt.%) and α-Zr (1.77(7) wt.%); (d) hydrogenated $Zr_3CoO_{0.6}$ alloy-constituent phases: $Zr_3CoO_{0.6}H_{5.95}$ (98.0(8) wt.%), $ZrCoH_x$ (1.6(2) wt.%) and ZrH_2 (0.5(3) wt.%).

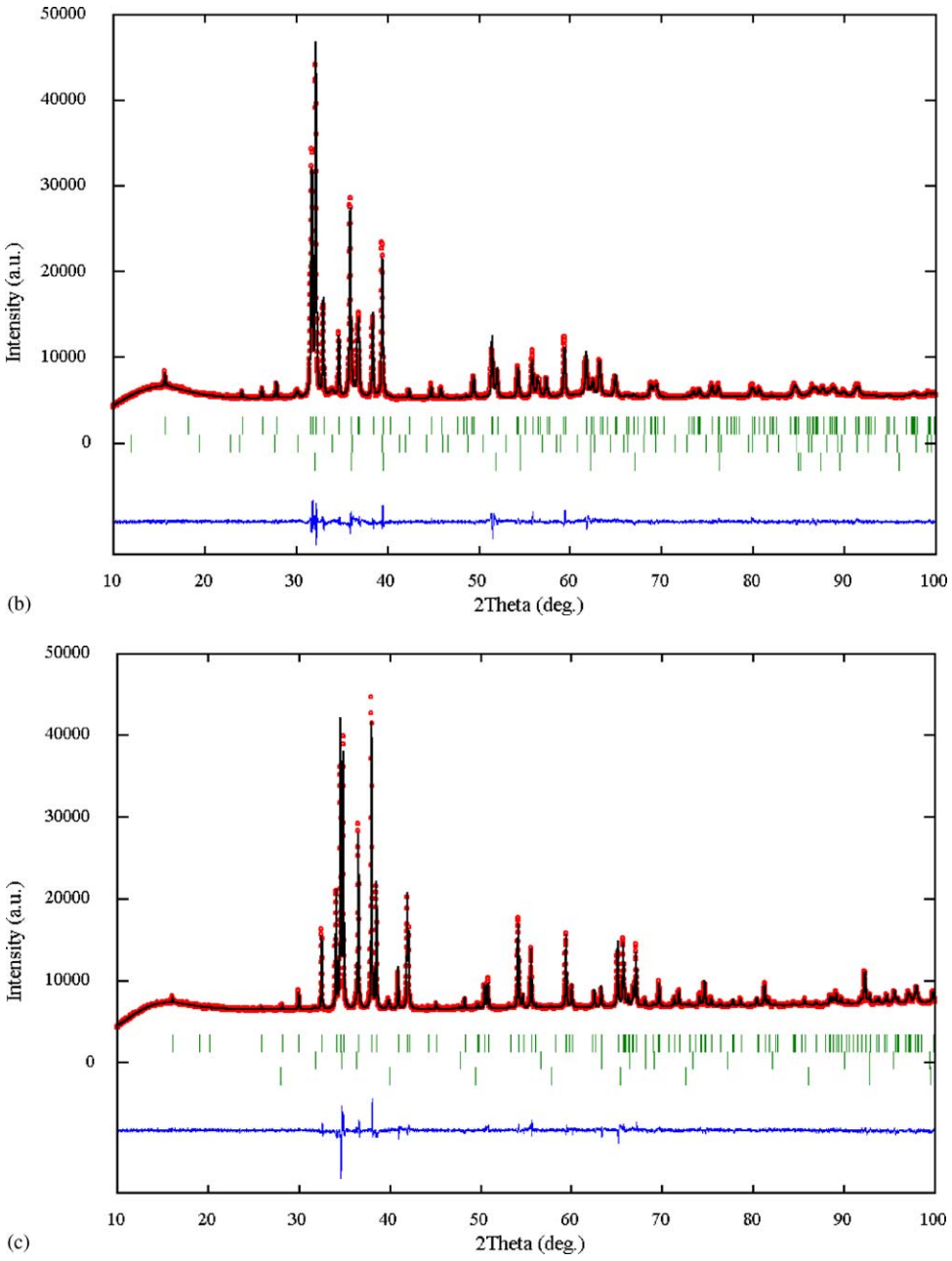

Fig. 2. (*Continued*)

The redistribution of oxygen atoms during hydrogenation of Zr_3MO_x (M = Fe, Co, Ni) compounds explains the unusual effect of a inverse dependence of the lattice expansion on the hydrogen storage capacity observed for these materials (see Fig. 1a and c).

The sample from the second batch containing the parent compound $Zr_3FeO_{0.4}$ was deuterated to the nominal composition $Zr_3FeO_{0.4}D_{6.5}$. The structure of this deuteride was characterised by the joint Rietveld refinement of the X-ray and neutron powder diffraction data (Fig. 3). The crystallographic parameters are collected in Table 3. A small impurity was observed in XRD and neutron powder pattern of the deuterated sample, but we were not successful in its identification. Four types of interstices occupied by deuterium atoms (one bi-pyramidal, D1, and three tetrahedral, D2–D4) were found in the crystal structure similar to those in the oxygen-free $Zr_3Fe(Co)D_x$ [3–5] and $Zr_3NiO_xD_y$ [7,8]. The only difference of the structure of $Zr_3FeO_{0.4}D_{6.5}$ from that of $Zr_3NiO_xD_y$ are the almost full occupancy of the D2 site and the absence of D atoms in the triangular Zr_3 sites (D5). It can be explained by a longer D2–D2 separation, which exceeds 2.0 Å in the iron containing deuteride. On the other hand, in Ni-containing deuterides the D2–D2 distances (∼1.74 Å) cause the partial occupation of this positions and a shift of a fraction of deuterium atoms in the D5 site (see [7] for more details).

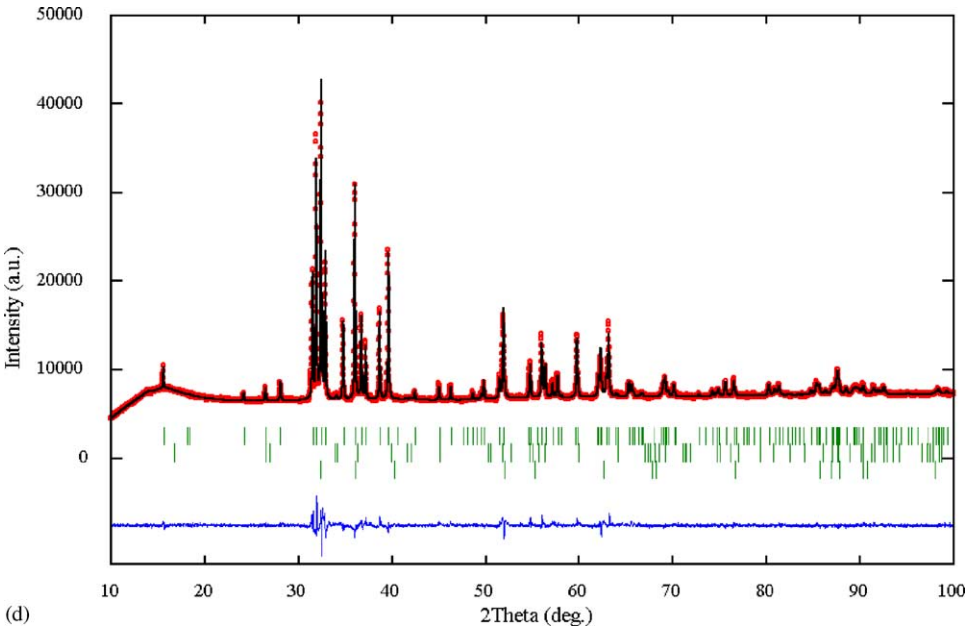

Fig. 2. (*Continued*).

3.2. ^{57}Fe Mössbauer spectroscopy and magnetic measurements

The effect of a hydrogen-induced appearance of magnetic order in $Zr_3FeO_{0.2}H_{6.25}$ and $Zr_3FeO_{0.6}H_{6.25}$ with respect to the paramagnetic parent compound $Zr_3FeO_{0.6}$ is shown in Fig. 4. The ordering temperatures are 105 and 140 K although the magnetic moments at 6 T are fairly low, 0.065 and 0.18 μ_B/f.u., respectively. Freezing effects appear at low temperatures as irreversibilities of the magnetisation upon zero field (ZFC) and field cooling (FC) which can be attributed to frustrated inter-grain exchange interactions but also to antiferromagnetic correlations within the grains (see below). It is worth to be noted that for $Zr_3FeO_{0.2}H_{6.25}$ an additional magnetic impurity phase is present which causes the non-vanishing magnetisation above T_C. Although the

Table 2
Atomic parameters of $Zr_3FeO_{0.6}$ and $Zr_3CoO_{0.6}$ compounds and their hydrides (space group Cmcm) from Rietveld refinement

Composition	Atom	Site	x	y	z	B_{iso} (Å^2)	G
$Zr_3FeO_{0.6}$	Zr1	4a	0	0.93547(9)	1/4	0.57(1)	1
	Zr2	8f	0	0.36235(7)	0.55992(8)	0.62(2)	1
	Fe	4c	0	0.2480(2)	1/4	0.57(4)	1
	O	4a	0	0	0	2.1(6)	0.62(2)
$R_{Bragg} = 3.95\%$; R_{wp} (corrected for background) $= 7.91\%$; $\chi^2 = 2.22$							
$Zr_3FeO_{0.6}H_{6.25}$	Zr1	4a	0	0.9185(1)	1/4	1.02(5)	1
	Zr2	8f	0	0.3604(1)	0.54914(9)	0.73(3)	1
	Fe	4c	0	0.2146(3)	1/4	1.54(8)	1
	O1	4a	0	0	0	2.0(–)	0.03(1)
	O2	8f	0	0.466(3)	0.362(3)	2.2(6)	0.24(1)
$R_{Bragg} = 4.23\%$; R_{wp} (corrected for background) $= 11.3\%$; $\chi^2 = 3.75$							
$Zr_3CoO_{0.6}$	Zr1	4a	0	0.9315(1)	1/4	0.30(4)	1
	Zr2	8f	0	0.3629(1)	0.5601(1)	0.44(3)	1
	Co	4c	0	0.2439(2)	1/4	0.46(7)	1
	O1	4a	0	0	0	1.3(7)	0.69(3)
$R_{Bragg} = 6.62\%$; R_{wp} (corrected for background) $= 12.5\%$; $\chi^2 = 3.79$							
$Zr_3CoO_{0.6}H_{5.95}$	Zr1	4a	0	0.9176(1)	1/4	0.86(5)	1
	Zr2	8f	0	0.3604(1)	0.5524(1)	0.26(3)	1
	Co	4c	0	0.2198(3)	1/4	1.9(1)	1
	O1	4a	0	0	0	2.0(–)	0.0(–)
	O2	8f	0	0.465(3)	0.361(3)	2.3(6)	0.27(1)
$R_{Bragg} = 6.14\%$; R_{wp} (corrected for background) $= 13.4\%$; $\chi^2 = 3.89$							

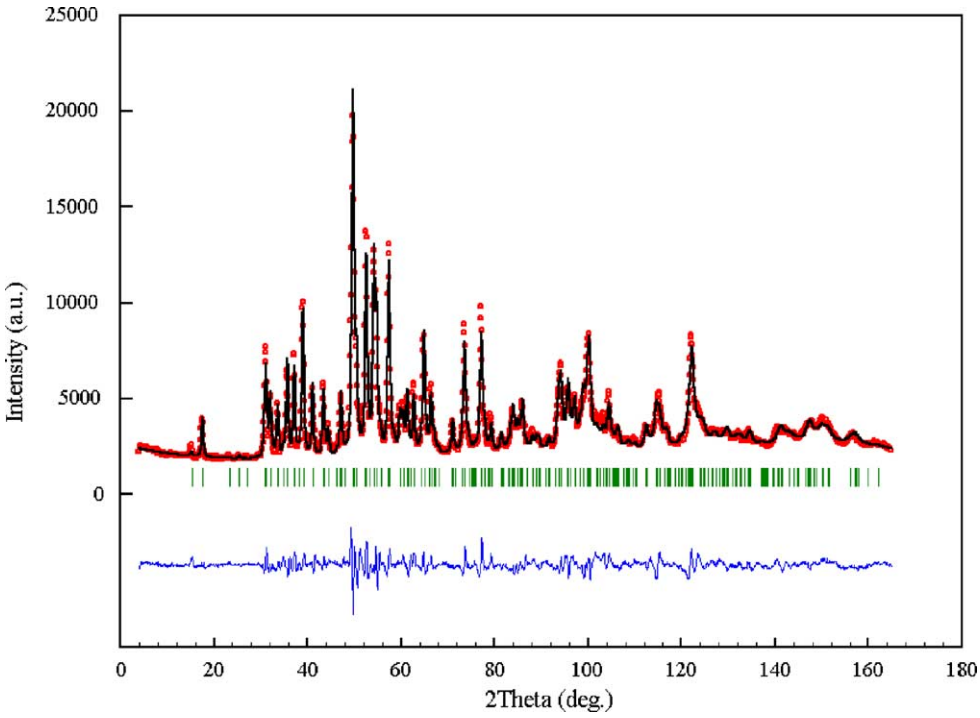

Fig. 3. Observed (points), calculated (line) and difference (lower line) neutron powder diffraction pattern for the $Zr_3FeO_{0.4}D_{6.5}$ deuteride. The vertical bars indicate the position of Bragg peaks.

parent compound $Zr_3FeO_{0.2}$ has not been investigated magnetically we suggest by analogy with $Zr_3FeO_{0.6}$ and Zr_3Fe that this compound is paramagnetic as well. The paramagnetic behaviour of the latter compounds can be characterised by the superposition of a temperature independent Pauli susceptibility χ_0 of about 1–3 $\times$ 10^{-6} emu/g and a weak Curie–Weiss susceptibility yielding an effective moment of about 0.2–0.4 μ_B/f.u. The wide range of χ_0 and the effective moment given arises from the remarkably strong field dependence of the susceptibility, which is largest for $Zr_3FeO_{0.6}$ over whole temperature range (2–300 K) but is also pronounced below 50 K for Zr_3Fe. The negative paramagnetic Curie temperatures of about −30 and −20 K for $Zr_3FeO_{0.6}$ and Zr_3Fe, respectively, are indicative for antiferromagnetic correlations within the grains, which may cause the irreversibilities and freezing effects in the susceptibility at about 7 K being observable up to 0.5 T and appear to be suppressed above. The comparison of the isothermal magnetisation in Fig. 5 indicates that oxygen insertion in Zr_3Fe causes a slight increase of the magnetisation and the curvature of $M(H)$ below 1 T while hydrogen absorption causes magnetic order (see Fig. 4). For the isostructural Co compounds—where $Zr_3CoO_{0.6}$ exhibits the lowest magnetisation at 2 K—hydrogen uptake increases the magnetisation and in particular the curvature of $M(H)$ below 2 T significantly but does not lead to long range magnetic order above 2 K in $Zr_3CoO_{0.6}H_{5.85}$, since the magnetic moment at 6 T corresponds to 0.011 μ_B/f.u. only. Accordingly, the susceptibility of $Zr_3CoO_{0.6}H_{5.85}$ is strongly field dependent and exhibits pronounced freezing effects at about 7 K.

Table 3
Atomic parameters of $Zr_3FeO_{0.4}D_{6.5}$ from the joint Rietveld refinement of X-ray and neutron powder patterns

Atom	Coordination[a]	x	y	z	U_{iso} ($\times 10^2$ Å^2)	G
Zr1 in 4c		0	0.9197(7)	1/4	1.0(1)	1.0(–)
Zr2 in 8f		0	0.3608(4)	0.5498(6)	0.71(9)	1.0(–)
Fe in 4c		0	0.2143(5)	1/4	1.2(1)	1.0(–)
O1 in 4a	O, $Zr1_2Zr2_4$	0	0	0	2.0(–)	0.01(2)
D1 in 4c	TB, $Zr1Zr2_2Fe_2$	0	0.7184(9)	1/4	1.8(2)	0.92(2)
D2 in 8f	Te, $Zr1Zr2_2Fe$	0	0.9118(6)	0.8550(6)	2.1(2)	0.94(2)
D3 in 8f	Te, $Zr1Zr2_3$	0	0.1721(5)	0.9449(7)	1.1(1)	0.99(2)
D4 in 8f	Te, $Zr1_2Zr2_2$	0	0.4633(6)	0.3722(6)	1.5(2)	0.8(1)
O2(D4) in 8f	Te, $Zr1_2Zr2_2$	0	0.4633(6)	0.3722(6)	1.5(2)	0.2(1)

Space group: Cmcm (no. 63); lattice parameters: a = 3.5482(3) Å, b = 11.238(1) Å, c = 9.718(1) Å, V = 387.50(7) Å^3; refined composition: $Zr_3FeO_{0.4}D_{6.44}$. R-factors: χ^2 = 15.1; R_{wp} = 14.4 − corrected for background; R_B = 4.51%.

[a] Coordination polyhedra of interstitial atoms (O, D): O = octahedral, TB = trigonal bi-pyramidal, Te = tetrahedral.

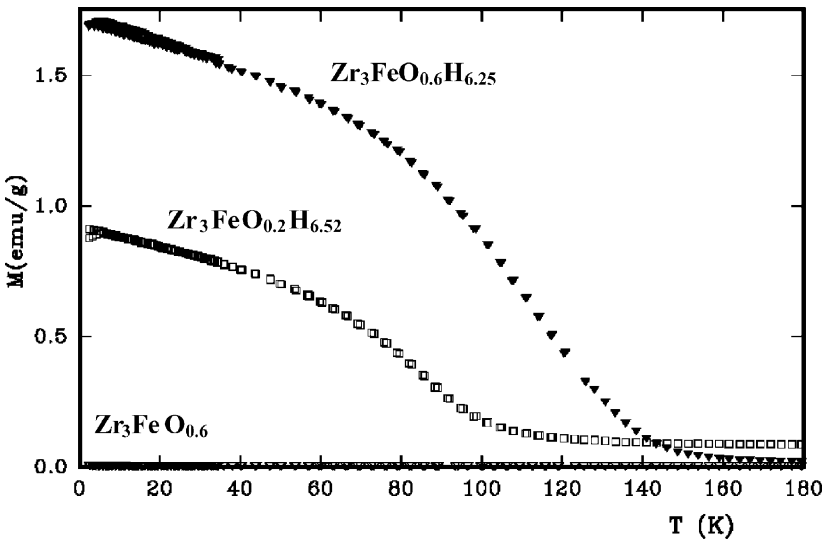

Fig. 4. Magnetisation as a function of temperature at $\mu_0 H = 0.1$ T.

The effective moment of about 2.2 μ_B/f.u together with a larger negative paramagnetic Curie temperature of −170 K is significantly larger than the parent $Zr_3CoO_{0.6}$ (0.2 μ_B, $\theta_p = -30$ K).

The ^{57}Fe Mössbauer effect was studied for three samples $Zr_3FeO_{0.6}$, $Zr_3FeO_{0.6}H_{6.25}$ and $Zr_3FeO_{0.2}H_{6.52}$. The spectra obtained from the three samples are shown in Fig. 6. The ^{57}Fe Mössbauer spectra of the $Zr_3FeO_{0.6}$ alloy can be fitted with two quadrupolar doublets with an area ratio of approximately 3:1. Since from X-ray diffraction studies only one Fe site per unit cell was determined the occurrence of two subpatterns can be due to either the presence of two chemical phases, which is unlikely because a second phase with an amount of about 25% should be visible in an X-ray diffraction pattern. Alternatively, the presence of two subspectra can be attributed to two different local environments of the Mössbauer nuclei, which is below the resolution of an X-ray experiment. To our experience this could be confirmed by an X-ray absorption study. Possibly, there is a non-uniform O-distribution within the crystal, leading to such large differences in the isomer shift. Compared to other intermetallic compounds the value of the quadrupole splitting (QS, see Table 4) is unusually large, reflecting a low symmetry at the Fe sites.

The quadrupole splitting increases slightly upon lowering the temperature from 295 to 4.2 K, indicating a small rise of the electric field gradient due to a decrease of the lattice dimensions. Even at 4.2 K no sign of a magnetic hyperfine splitting can be observed in the spectrum recorded from parent $Zr_3FeO_{0.6}$.

The room temperature spectra taken from both hydrides $Zr_3FeO_{0.6}H_{6.25}$ and $Zr_3FeO_{0.2}H_{6.52}$ consist of one weakly resolved quadrupole split doublet, indicating a small electric field gradient compared to that present in the parent

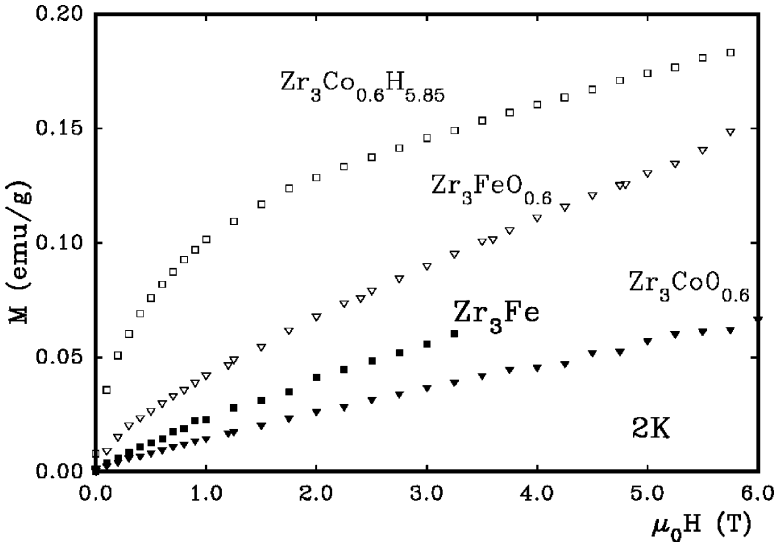

Fig. 5. Magnetisation as a function of field at 2 K.

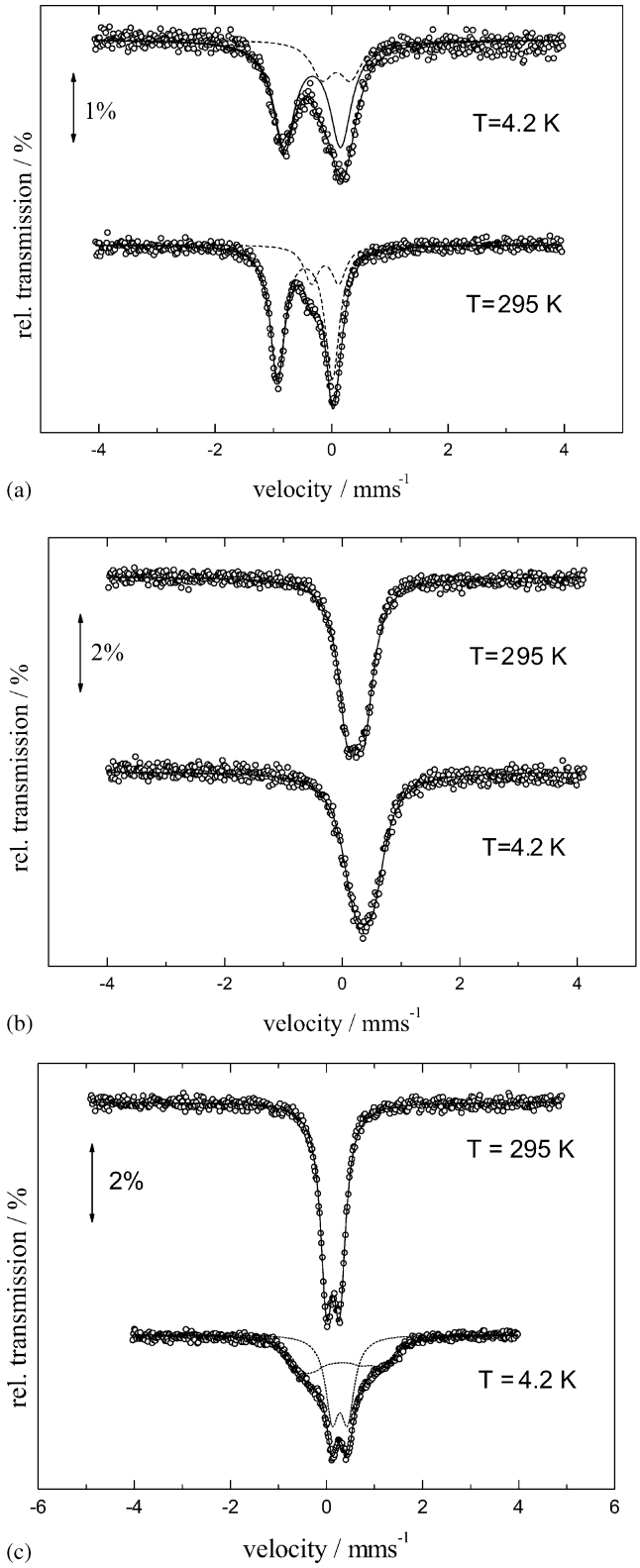

Fig. 6. Mössbauer spectra of $Zr_3FeO_{0.6}$ (a), $Zr_3FeO_{0.6}H_{6.25}$ (b) and $Zr_3FeO_{0.2}H_{6.52}$ (c).

Table 4
Fitted parameters of Mössbauer spectra

	$Zr_3FeO_{0.6}$		$Zr_3FeO_{0.6}H_{6.25}$		$Zr_3FeO_{0.2}H_{6.52}$	
Temperature (K)	4.2	295	4.2	295	4.2	295
IS (mm/s)	−0.33	−0.46	0.36	0.23	0.29	0.14
	0.08	−0.11			0.28	
QS (mm/s)	0.97	0.94	0.00	0.28	0.08	0.27
	0.49	0.47			0.32	
B_{hf} (T)	0.00	0.00	1.26	0.00	5.16	0.00
	0.00	0.00			0.00	
Area (%)	74.37	78.27	100	100	53.90	100
	25.63	21.73			46.10	

compound, possibly due to screening effects caused by hydrogen. Huge changes in isomer shift (IS) from negative to positive values are obtained upon hydrogen uptake, larger than commonly observed for metal–hydrogen systems. The large increase in isomer shift upon hydrogen absorption up to $0.7\,mm\,s^{-1}$ cannot only be attributed to the rise of the cell volume. A appreciable s-like charge transfer from Fe is supposed to occur as well, leading to a significantly reduced s-electron density at the Mössbauer nucleus.

At liquid helium temperature for both hydrides a magnetic hyperfine field is observed. For $Zr_3FeO_{0.2}H_{6.52}$ both a Zeeman and quadrupole split pattern is obtained with almost equal absorption area. This, again, points to the sensitivity of the hyperfine interactions upon the local environment. From the shape of the Mössbauer spectrum we suggest that two sets of a near neighbour environment of the Mössbauer nuclei are present, particularly differing in the number of Fe neighbours. The hyperfine field is rather weak indicating the occurrence of a weak hydrogen-induced magnetic ordering at low temperatures. In the case of $Zr_3FeO_{0.6}H_{6.25}$, at 4.2 K, a symmetric broadened line is observed, indicating the absence of a quadrupole splitting. A reasonable fit to the experimental data can only be performed, if the presence of a small hyperfine field is assumed. Its magnitude, derived from fitting the data is even less than that obtained for $Zr_3FeO_{0.2}H_{6.52}$ (see Table 4).

Since the Mössbauer experiment for $Zr_3FeO_{0.2}$ has not yet been performed we can assume the absence of any magnetic ordering in this compound from taking into account the results obtained for $Zr_3FeO_{0.6}$ and the Mössbauer data for Zr_3Fe reported previously by Aubertin et al. [6].

4. Conclusions

It has been shown that the oxygen-stabilised compounds $Zr_3Fe(Co)O_x$ ($x = 0$–1.0) form saturated hydrides with filled Re_3B type structure. The insertion of oxygen atoms in the crystal structure results in minor changes of the unit cell volumes of Zr_3FeO_x or to its slight decrease for Zr_3CoO_x. A substantial increase of these parameters for the corresponding saturated hydrides has been observed with

increasing oxygen content, whereas, the H-storage capacity decreased from 6.7 H/f.u. for Zr_3Fe down to 5.35 H/f.u. for $Zr_3FeO_{1.0}$ and from 6.9 H/f.u. for Zr_3Co down to 5.3 H/f.u. for $Zr_3CoO_{1.0}$. Joint Rietveld refinement of X-ray and neutron powder diffraction data for $Zr_3FeO_{0.4}D_{6.25}$ has shown a similar distribution of deuterium atoms and a redistribution of oxygen atoms from octahedral to tetrahedral sites as it was observed for $Zr_3NiO_xD_y$ [7]. The inverse dependence of the lattice expansion on the hydrogen storage capacity is observed for all studied Zr_3MO_x (M = Fe, Co, Ni) compounds. This behaviour for $Zr_3NiO_xD_y$ has been supposed as a result of the redistribution of oxygen atoms during hydrogenation and the obtained results could be considered as an additional argument for it.

At liquid helium temperature both hydrides $Zr_3FeO_{0.2}H_{6.52}$ and $Zr_3FeO_{0.6}H_{6.25}$ a weak magnetic hyperfine field is observed, indicating the occurrence of hydrogen-induced magnetic ordering at low temperatures. Also the hydrogen-induced magnetic order in $Zr_3FeO_{0.2}H_{6.25}$ and $Zr_3FeO_{0.6}H_{6.25}$ (with respect to the paramagnetic parent compounds $Zr_3Fe(Co)O_x$) with the ordering temperatures at 105 and 140 K, respectively, has been determined by magnetic susceptibility measurements.

Acknowledgements

The help of Ya. Filinchuk (University of Geneva) and of Denis Sheptyakov (PSI) with the neutron powder diffraction experiment is appreciated. Part of this work was carried out in the frame of INTAS Fellowship grant for Young Scientists (Dr. R. Denys) YSF 2002-428. Dr. I. Zavaliy thanks International Center of Diffraction data (ICDD) for the support of X-ray structural studies.

References

[1] H. Boller, Monatch. Chem. 104 (1973) 545–551.
[2] R. MacCay, H.F. Franzen, J. Alloys Comp. 186 (1992) L7–L10.
[3] V.A. Yartys, H. Fjellvåg, I.R. Harris, J. Alloys Comp. 293–295 (1999) 74–87.
[4] V.A. Yartys, H. Fjelvåg, B.C. Hauback, A.B. Riabov, M.H. Sørby, J. Alloys Comp. 278 (1998) 252–259.
[5] A.B. Riabov, V.A. Yartys, H. Fjelvåg, B.C. Hauback, M.H. Sørby, J. Alloys Comp. 296 (1–2) (2000) 312–316.
[6] F. Aubertin, G.L. Whittle, S.J. Campbell, U. Gonser, Phys. Stat. Sol. (a) 104 (1987) 397–402.
[7] I.Yu. Zavaliy, R. Černý, I.V. Koval'chuck, I.V. Saldan, J. Alloys Comp. 360 (2003) 173–182.
[8] I. Zavaliy, R. Černý, I. Koval'chuck, A. Riabov, Visnyk Lviv. University, Ser. Khim. 43 (2003) 48–52.
[9] L.G. Akselrud, Yu.N. Grin, P.Y. Zavalii, V.K. Pecharsky, B. Baumgartner, E. Wolfel, Use of the CSD program package for structure determination from powder data, in: Proceedings of the Second European Powder Diffraction Conference: Abstract of Papers, Enschede, The Netherlands, 1992, p. 41;
L.G. Akselrud, Yu.N. Grin, P.Y. Zavalii, V.K. Pecharsky, B. Baumgartner, E. Wolfel, Mater. Sci. Forum (1993) 133–136, 335–340.
[10] J. Rodríguez-Carvajal, Program FullProf.2k, Version 2.20, Laboratoire Léon Brillouin (CEA–CNRS), France, 2002.